Magnetism and phase stability of fcc Fe-Co alloys precipitated in a Cu matrix

2001 J. Phys.: Condens. Matter 13 6359

(http://iopscience.iop.org/0953-8984/13/29/306)

INSTITUTE OF PHYSICS PUBLISHING JOURNAL OF PHYSICS: CONDENSED MATTER

J. Phys.: Condens. Matter **13** (2001) 6359–6369 PII: S0953-8984(01)25089-9

Magnetism and phase stability of fcc Fe–Co alloys precipitated in a Cu matrix

M Shiga and M Yamamoto

Department of Materials Science and Engineering, Kyoto University, Kyoto 606-8501, Japan

Received 21 May 2001
Published 6 July 2001
Online at stacks.iop.org/JPhysCM/13/6359

Abstract

The magnetism and phase stability of Fe-rich fcc Fe–Co alloys precipitated in a Cu matrix were studied by measuring the magnetization in the *in situ* condition during a precipitation heat treatment for the sample of $Cu_{98}(Fe_{1-x}Co_x)_2$ ($x \leqslant 0.55$). It was found that fcc Fe–Co becomes ferromagnetic for $x > 0.4$. The Curie temperature and the spontaneous magnetization were determined. They exhibit a similar concentration dependence to fcc Fe–Ni alloys, indicating Invar phenomena at the critical concentration. By observing the thermal hysteresis of magnetization change for various heat sequences the fcc-to-bcc transition was detected for $x > 0.3$ and its transition temperature was determined. The stability of the fcc phase was discussed in terms of the lattice misfit and the Invar effect.

1. Introduction

Fe-rich Fe–Co alloys are widely used as ferromagnetic materials with the largest magnetization at room temperature. The equilibrium crystal structure of the alloy is body-centred-cubic over a wide concentration range up to 70 at% Co. Recent developments in producing non-equilibrium phases of alloys may allow us to obtain Fe–Co alloys with another crystal structure such as fcc. In fact, it was reported that epitaxially deposited Fe–Co thin films on a Cu(001) face show fcc structure over all concentration ranges (Zharnikov *et al* 1996). These films exhibit a fairly large magneto-optical Kerr effect at room temperature indicating the ferromagnetism of the alloys. Ambrose *et al* (1999) have shown that Fe_xCo_{1-x} films deposited on diamond (100) substrates are also ferromagnetic and have fcc structure over all the concentration range. They measured the magnetization of the films and have revealed that even pure fcc Fe is ferromagnetic with a large saturation moment and the magnetization decreases with increasing Co content. There are many data on the magnetism of epitaxial Fe films, some of which claim that the ground state of fcc Fe is antiferromagnetic (Macedo and Keune 1988). The magnetic state of fcc Fe is unstable and is very sensitive to substrates and conditions of preparation.

Coherent precipitation of Fe or Fe–Co from the Cu matrix can also provide the fcc phase. There are a tremendous number of works on fcc(γ)-Fe produced by precipitation. It is believed

that γ-Fe thus obtained is antiferromagnetic with small ($\mu_{Fe} < 1\ \mu_B$) magnetic moment and $T_N \sim 70$ K. However, precise diffraction studies by Tsunoda and Kunitomi (1988) have revealed that γ-Fe precipitates undergo considerable lattice deformation accompanied by antiferromagnetic ordering except an early stage of the precipitation. One of the authors (MS) showed that Fe–Co precipitates in a Cu matrix also retains the fcc structure forming Fe–Co alloys with nearly the same Co fraction as the nominal composition of $Cu_{98}(Fe_{1-x}Co_x)_2$ mother alloys (Nakamura *et al* 1969). This phenomenon is based on the facts that: (1) Fe and Co are very soluble together but not in Cu; and (2) the phase diagrams of Cu–Fe and Cu–Co alloys are quite similar and the solubility limits of both elements are also nearly the same; a few per cent just below the melting points and less than 1% at around 900 K where a heat treatment for precipitation is performed. They have shown that fcc $Fe_{1-x}Co_x$ alloys remain non-magnetic in a Fe-rich region and become ferromagnetic around $x > 0.2$. More extensive work was done by the same group using Mössbauer spectroscopy (Muraoka *et al* 1981). They have revealed that the alloys are antiferromagnetic with small magnetic moment for $x < 0.3$ and a sharp transition to a ferromagnet with the full moment of 3d metals takes place around $x = 0.3$. They have also shown that the fcc lattice becomes unstable to bcc structure with increasing the Co content, in particular for $x > 0.45$. This sounds somewhat peculiar because in the binary Fe–Co system the fcc phase appears in the Co-rich region. Since then, a few works on fcc Fe–Co alloys have been done by other groups. Tsunoda (1988, 1989) has revealed by x-ray and neutron diffraction studies that an introduction of a small amount of Co suppresses the structural phase transition of γ-Fe precipitates in Cu and the cubic γ-Fe–Co alloys are available even at the lowest temperature. They have also shown that the magnetic structure of the cubic γ-$Fe_{1-x}Co_x$ alloys ($x < 0.04$) is a spin density wave state, whose Néel temperature and the SDW wavelength decrease with Co concentration. Monzen *et al* (1989, 1992) studied the stability of the fcc phase Fe–Co precipitates in Cu and discussed the mechanism of the martensitic transformation of the alloys from the metallurgical points of view. They confirmed that the fcc phase becomes less stable with increasing Co concentration.

In previous works on Fe–Co precipitates in Cu, most of the measurements were carried out for the samples which were subjected to heat treatments for precipitation. They inevitably contain more or less bcc precipitates, particularly in Co-rich alloys. Since both fcc and bcc precipitates are ferromagnetic for $x > 0.3$, it is difficult to know the magnetic properties of ferromagnetic fcc Fe–Co in the Co-rich region. In this study, we carried out the magnetization measurements in the *in situ* condition during a precipitation heat treatment. This enable us to determine the magnetization and the Curie temperature of fcc Fe–Co and the phase boundary of the fcc-to-bcc transformation in the precipitates.

2. Experimental procedures

Ingots of $Cu_{98}(Fe_{1-x}Co_x)_2$ alloys were prepared by an induction furnace in a high purity argon atmosphere. 99.99% pure Cu, 99.9% pure Fe and Co metals were used as raw materials. In order to achieve good homogeneity, the alloys were kept for 30 min above their melting point in the furnace. The ingot was cut into small thin plates with about 0.5 mm thickness and 0.05 g weight to achieve a rapid cooling of the sample during iced water quenching. These plate samples were sealed into an evacuated quartz tube and subjected to homogenizing and solution heat treatments at 1323 K for 1 h. They were then rapidly quenched into iced water by breaking the capsule in the water.

A specimen thus obtained was set into the quartz sample holder of vibrating-sample-magnetometer (Toei VSM-5). The chamber of the VSM was evacuated to 10^{-4} Torr to avoid

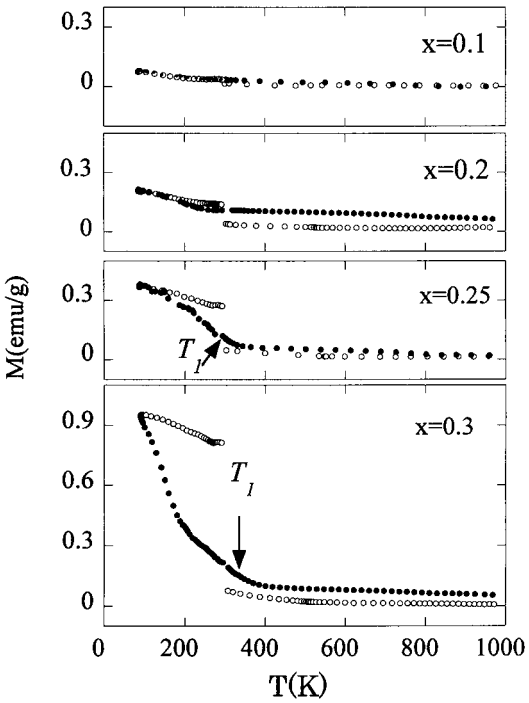

Figure 1. Variation of magnetization of $Cu_{98}(Fe_{1-x}Co_x)_2$ for $0.1 \leqslant x \leqslant 0.3$ during the standard thermal sequence. Open circles, heating process; closed circles, cooling process. Arrows indicate the temperature where the magnetization increases rapidly with decreasing temperature (T_1).

oxidation of the sample. The magnetization of the sample at 0.5 T was measured during a thermal sequence which accelerated the precipitation of the Fe–Co alloy from the Cu matrix. Digitized output of VSM and thermocouple was stored in a PC during this heat sequence through GPIB. The standard thermal sequence is as follows: (1) rapid heat up to 973 K in 20 min; (2) keep 973 K for 120 min, gradually cool down to room temperature in 120 min; (3) cool down to liquid nitrogen temperature; and (4) finally heat up to room temperature. It was reported that Fe precipitates in Cu are nearly spherical and the growth of particle size, r, as a function of annealing time, t, is given by $r^3 = kt$ (Watanabe *et al* 1991). They estimated $k = 3.9 \times 10^{-28}$ m^3 s^{-1} for 973 K by electron microscopy study. Assuming that this value is applicable to Fe–Co precipitates, we can expect a particle size of about 15 nm for this standard sequence. Apart from the standard sequence, many other variations of sequences were carried out in order to know the reversibility of magnetization change for increasing and decreasing temperature, which may make it possible to distinguish the origin of the magnetization change between the ferromagnetic ordering and the fcc–bcc phase transition and the effect of particle size on the magnetic and structural transition temperatures.

3. Results and discussion

3.1. Magnetization change for the standard thermal sequence

Figure 1 shows the variation of magnetization during the standard thermal sequence for $0.1 \leqslant x \leqslant 0.3$. For $x = 0.1$, almost no change was observed before and after the annealing at

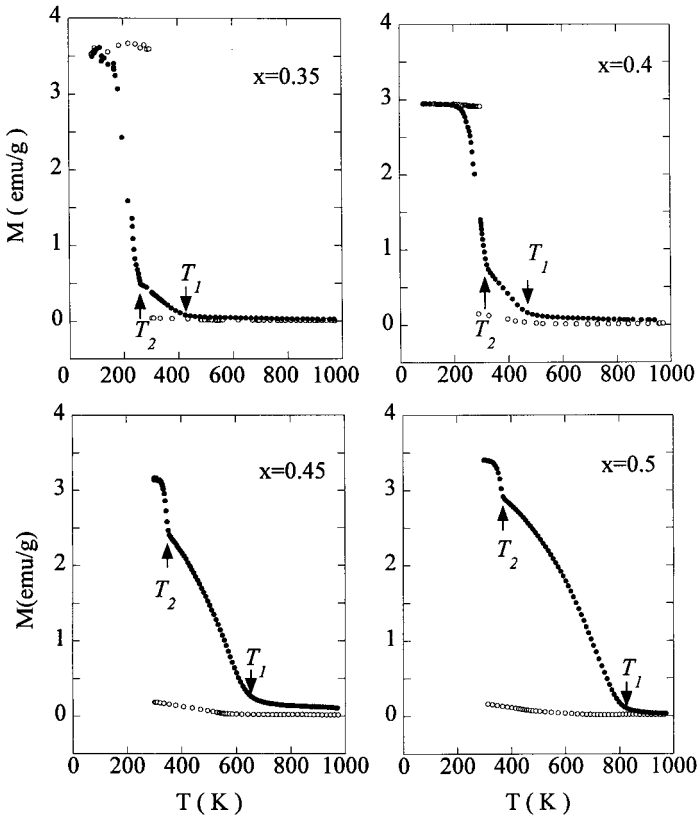

Figure 2. Variation of magnetization of $Cu_{98}(Fe_{1-x}Co_x)_2$ for $0.35 \leqslant x \leqslant 0.5$ during the standard thermal sequence. Open circles, heating process; closed circles, cooling process. Arrows indicate the temperature where the magnetization increases rapidly with decreasing temperature (T_1 and T_2).

973 K, indicating that the precipitates are fcc and paramagnetic down to the lowest temperature. The profile for $x = 0.2$ is nearly the same as for $x = 0.1$ except for a small increase of magnetization after the annealing at 973 K. This increase of magnetization during the annealing is probably due to the partial transformation of precipitates into the bcc phase. However, its magnitude is not reproducible and does not systematically depend on the concentration as seen in the figure. Presumably, it depends on the condition of the quenching which is not rapid enough to obtain a complete solid solution but allows the formation of atomic clusters. We found a trend that the more perfect quenching gives a smaller increase at 973 K. For $x = 0.25$, the increase of magnetization at low temperatures (indicated by T_1) becomes a little more distinct than that for $x = 0.2$ and an irreversibility was observed in magnetization for the final heating process. These behaviours become more clear in the magnetization against temperature (M–T) curve for $x = 0.3$. Figure 2 shows M–T curves of $Cu_{98}(Fe_{1-x}Co_x)_2$ for $0.35 \leqslant x \leqslant 0.5$. It can clearly be seen that the magnetization abruptly increases in two steps at T_1 and T_2 for the cooling process after 973 K annealing. The position of T_1 shifts to the right-hand (high temperature) side with increasing Co fraction while that of T_2 remains almost constant.

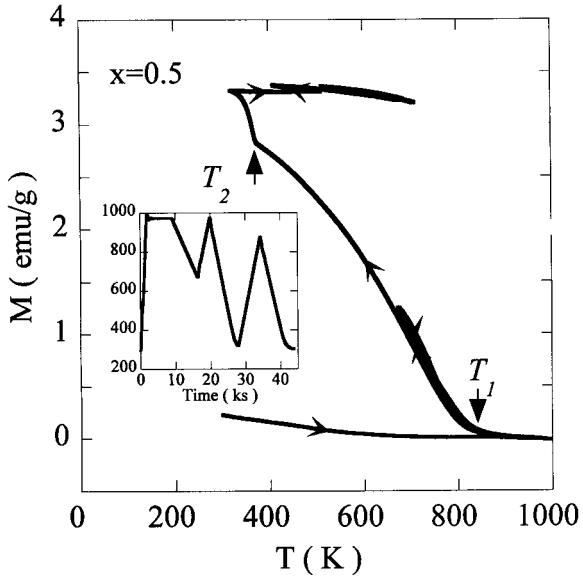

Figure 3. Variation of magnetization of $Cu_{98}(Fe_{0.5}Co_{0.5})_2$ against temperature for the thermal sequence indicated in the inset.

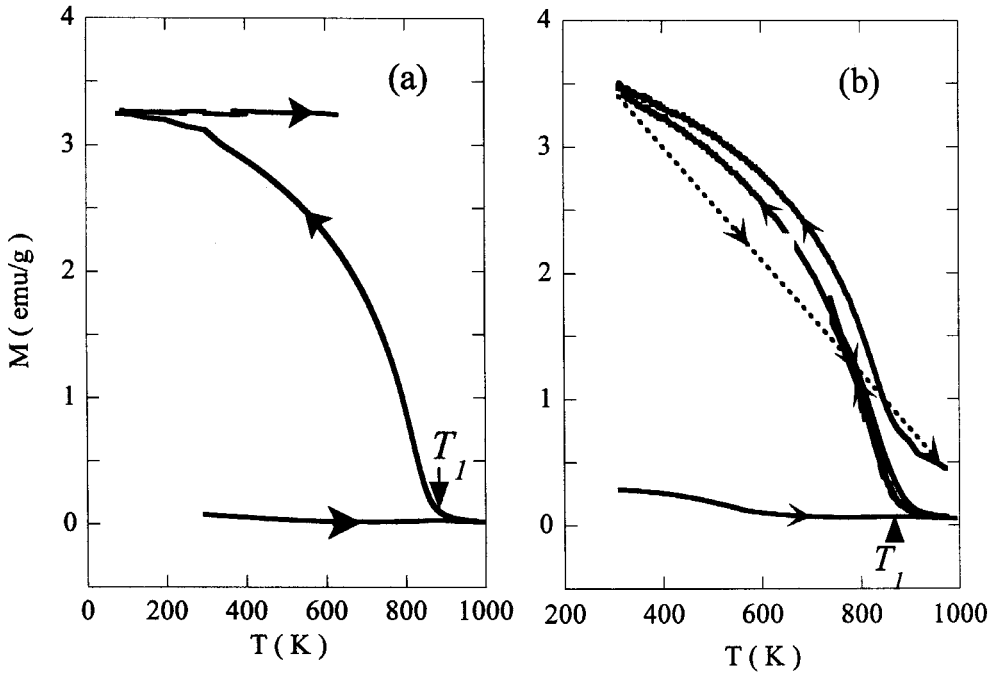

Figure 4. Variation of magnetization of $Cu_{98}(Fe_{0.45}Co_{0.55})_2$ against temperature for (a) the standard thermal sequence and (b) heat cycles above room temperature.

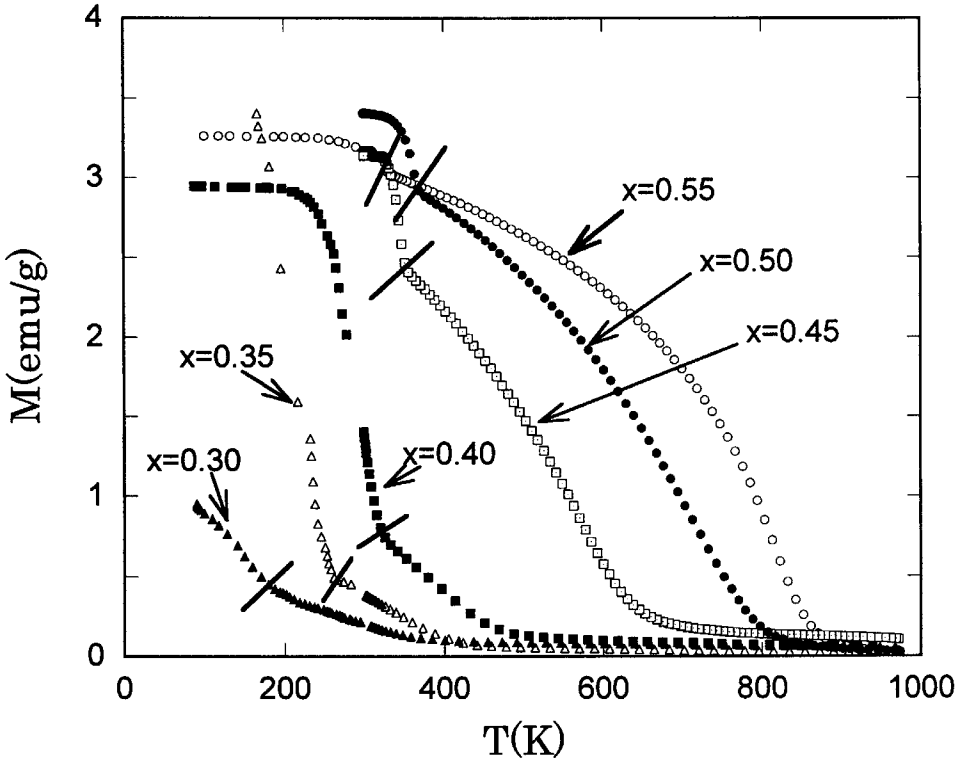

Figure 5. Magnetization against temperature of $Cu_{98}(Fe_{1-x}Co_x)_2$ for the cooling process after 973 K ageing. Bold lines indicate the starting point of the fcc-to-bcc transition.

3.2. Reversibility of magnetization change against temperature: origins of the magnetization jump

In order to know the origin of these two characteristic temperatures, we measured the magnetization change of the $x = 0.5$ sample for the thermal sequence as shown in the inset of figure 3 and carefully examined the thermal reversibility of the magnetization change around T_1 and T_2. The result of this measurement is shown in figure 3. It becomes evident that the rapid increase of magnetization below T_1 is perfectly reversible against temperature, suggesting that T_1 corresponds to the Curie temperature of the precipitates. Noting the fact that T_1 rapidly increases with x and appears to coincide with the Curie temperature of fcc Fe–Co alloys in the Co-rich equilibrium phase (as indicated in figure 7, later) we can conclude that T_1 represents the Curie temperature of the Fe–Co precipitates. On the other hand, the rapid increase of magnetization with decreasing temperature at T_2 does not reversibly decrease with increasing temperature, indicating that the precipitates transformed to the bcc phase, which has a high Curie temperature. Hereafter, we denote T_1 as T_c, the Curie temperature of the fcc phase, and T_2 as T_t, the transformation temperature from fcc-to-bcc structure.

The M–T curve for $x = 0.55$ exhibits somewhat different behaviours from others. Figure 4(a) shows the M–T curve of the standard sequence. We observed only T_1 but not T_2. However, it is clear that the fcc-to-bcc transition took place at a low temperature, which is not observed as a rapid increase of magnetization (T_2). On the other hand, the M–T curve for a heat cycle above room temperature is nearly reversible. These observations indicate

that the fcc-to-bcc transformation of precipitates occurs below room temperature, while the magnetization jump is not observed because of a large enough magnetization of fcc phase due to the high Curie temperature. This means that the spontaneous magnetization at 0 K is almost the same for fcc and bcc Fe–Co alloys in this concentration.

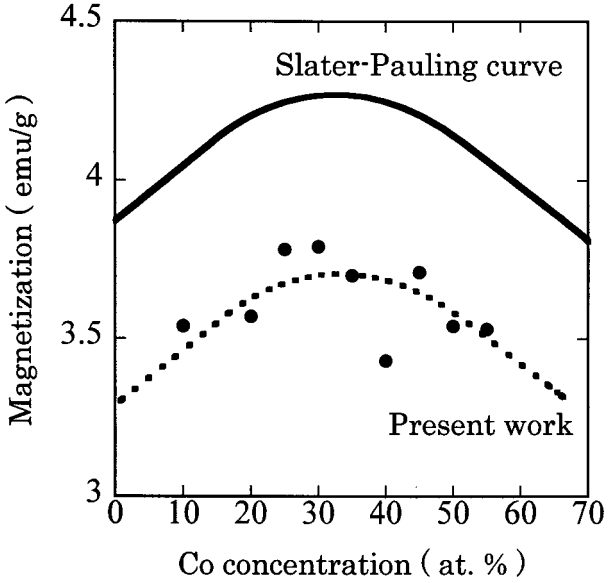

Figure 6. Magnetization of $Cu_{98}(Fe_{1-x}Co_x)_2$ after mechanical working. Fe–Co precipitates should be transformed into the bcc phase. The full curve indicates the expected magnetization for 2% bulk bcc Fe–Co dispersed in pure Cu. The broken curve is a guide for the eyes.

3.3. Magnetic properties of fcc Fe–Co alloys

We have already seen that the fcc-to-bcc transition mostly takes place in a cooling process after 973 K ageing except for a tiny amount of bcc precipitates which are transformed during the ageing process at 973 K. Figure 5 shows the magnetization against temperature curves of $Cu_{98}(Fe_{1-x}Co_x)_2$ for the cooling process. M–T curves above the fcc-to-bcc transition temperature, which are indicated by bold lines, are roughly regarded as the M–T curve of fcc Fe–Co alloys. The small residual magnetization, M_r, above T_c, however, indicates the spontaneous magnetization of bcc precipitates which have a high Curie temperature. Therefore, we define the magnetization of the fcc phase as $M_{fcc}(T) = M_{obs}(T)$–M_r. For M_r, we take a constant value of the magnetization just above T_c. Accurate values of T_c for the fcc phase are determined by a M^2_{fcc} against T plot for each sample. Furthermore, the spontaneous magnetizations of fcc Fe–Co at 0 K are estimated by fitting the M_{fcc}–T curves to the calculated M–T curve obtained from the molecular field theory for the $S = 1$ Brillouin function. In order to obtain the spontaneous atomic moment of the fcc Fe–Co system, however, we have to take into consideration of the fact that a part of the Fe and Co still remain as solutes in the Cu matrix. To estimate the fraction of Fe and Co included in precipitates, we noted the phenomenon that mechanical working, say simply hitting the samples with a steel hammer, forces fcc precipitates to transform to the bcc phase (see, e.g., Muraoka *et al* (1981)). Figure 6 shows the magnetization of the $Cu_{98}(Fe_{1-x}Co_x)_2$ sample at 77 K after being subjected to mechanical work. The expected magnetizations of $Cu_{98}(Fe_{1-x}Co_x)_2$ are shown in this figure

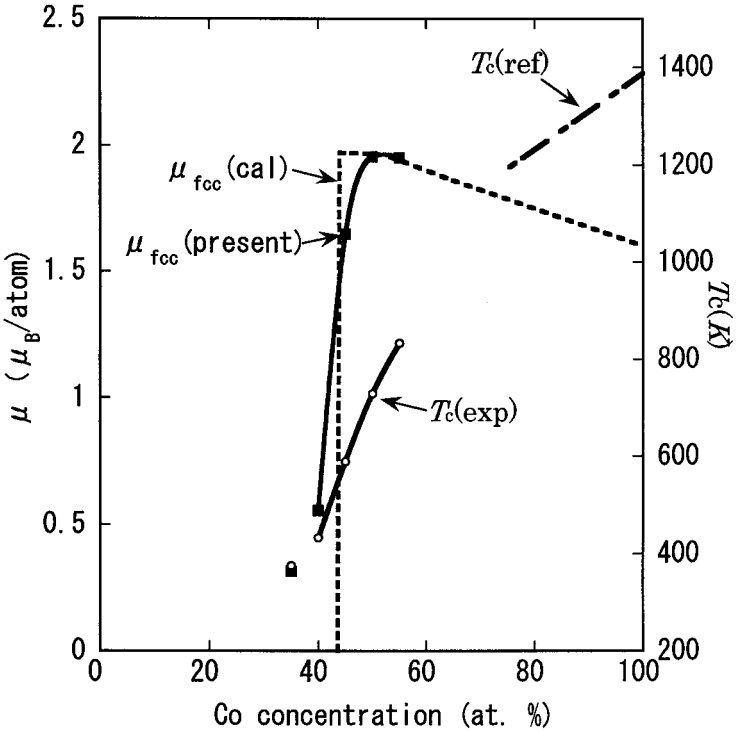

Figure 7. Full squares are the mean atomic moment of the fcc Fe–Co alloys. The full curve is a guide for the eyes. The broken curve is theoretical value after Abrikosov *et al* (1996). Open circles are the Curie temperature of the fcc Fe–Co. The dots and dashes line represents the Curie temperature of the fcc Fe–Co in the equilibrium phase.

assuming that Fe and Co atoms perfectly precipitate as bcc $Fe_{1-x}Co_x$ alloys. Although the data points are somewhat scattered, we can conclude that (1) about 85% of the Fe–Co is included in precipitates and (2) the concentrations of the precipitates are nearly the same with the nominal compositions of Fe and Co. Then, it is possible to estimate the spontaneous atomic moment of the fcc Fe–Co system, results of which are shown in figure 7 together with the theoretical values obtained from the CPA-LMTO-ASA method (Abrikosov *et al* 1996) and the Curie temperature. Agreement with the theoretical estimation of the mean magnetic moment is surprisingly good, probably accidentally. Anyway, the sharp drop of the spontaneous moment at around 40%Co ($e/a = 8.8$) and the rapid decrease of the Curie temperature with increasing Fe content are just characteristics of the Invar type alloys such as Fe–Ni and Fe–Ni–Mn systems (Shiga 1993). Therefore, the so-called Invar type thermal expansion anomaly would be expected in the present alloys. As discussed in the next section, this behaviour may be responsible for the lattice stability of the fcc phase.

3.4. Lattice stability of fcc Fe–Co precipitates

Figure 8 indicates the fcc-to-bcc transition temperature T_t of the Fe–Co precipitates. As pointed out in a previous paper (Muraoka *et al* 1981), the fcc structure becomes less stable with increasing Co content. In fact, it becomes evident that the fcc phase is stable down to the lowest temperature for $x < 0.3$ and T_t increases with increasing Co content up to $x = 0.5$

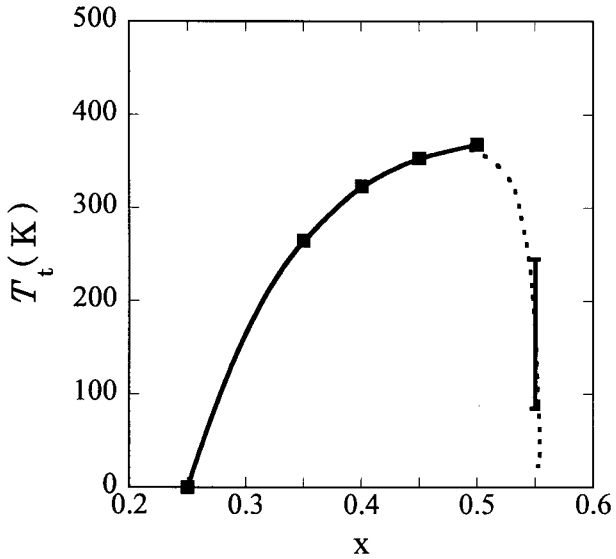

Figure 8. Concentration dependence of the fcc-to-bcc transformation temperature of $Fe_{1-x}Co_x$ precipitates.

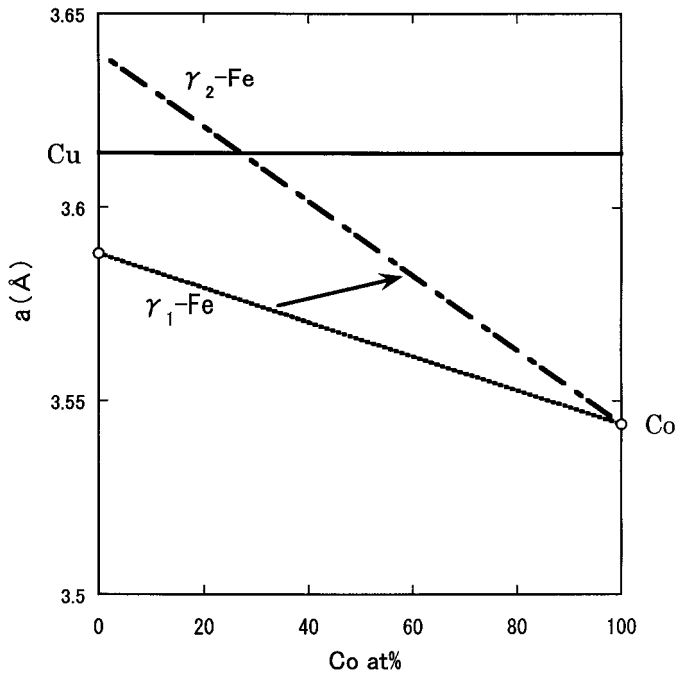

Figure 9. Expected lattice constants of the fcc Fe–Co alloy at room temperature for low-spin (γ_1) and high-spin state (γ_2) Fe assuming Vegard's law. The horizontal line indicates the lattice constant of Cu. A bold arrow indicates a change of lattice constant accompanied with the γ_1 to γ_2 transformation.

in accordance with the previous observation. However, in the present study, we found that T_t exhibits a maximum at around $x = 0.5$ and decreases again above $x = 0.5$ indicating the re-stabilization of the fcc structure. Naively it seems peculiar that the fcc phase becomes less stable with increasing Co content because, in the equilibrium phase diagram, the stable fcc phase appears on the Co-rich side.

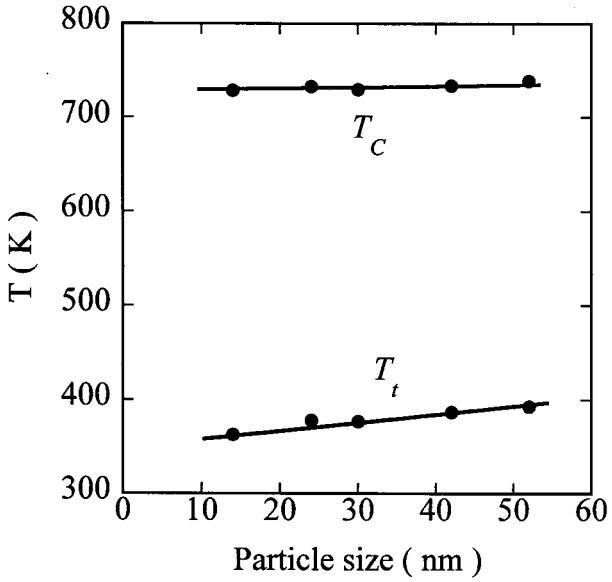

Figure 10. Particle size dependence of the Curie temperature, T_c and the fcc-to-bcc transition temperature, T_t for the $x = 0.5$ sample.

We can explain this behaviour as the result of the change in degree of the lattice misfit as follows. Figure 9 shows the expected lattice constant of fcc Fe–Co from Vegard's law for the high-spin (γ_2) and the low-spin (γ_1) states of γ-Fe (Weiss 1963) together with that of Cu, where the lattice constant of γ_1-Fe was directly measured by Tsunoda *et al* (1988) for precipitated fcc iron. As seen in the figure, the lattice constant of pure γ-Fe is a little smaller than that of Cu and the difference becomes larger with increasing Co content as long as Fe remains in the low spin state, implying that the coherency between fcc precipitates and the Cu matrix becomes less stable. However, in the ferromagnetic region, we can expect that Fe atoms approach the γ_2-state and the lattice constant transfers to Vegard's law for γ_2-Fe and fcc Co as indicated in the figure, resulting in the decrease of the lattice misfit and the re-stabilization of the fcc phase. This means that fcc Fe–Co should exhibit the Invar-type thermal expansion anomaly (Shiga 1993) in the concentration range around 50% Co, although it is not easy to observe directly the thermal expansion anomaly of the precipitates.

3.5. Particle-size dependence of characteristic temperatures

So far, the precipitation treatment was performed under the same conditions at 973 K for 120 min for every experiment, resulting in nearly the same particle size of precipitates of about 15 nm. We have examined the particle size dependence of the two characteristic temperatures, T_c and T_t for the $x = 0.5$ sample by changing the annealing temperature at 973 K. The results are shown in figure 10, where the particle size was estimated by using the equation

given in section 2. It becomes evident that the Curie temperature is almost constant against the size, indicating that T_c is intrinsic for fcc Fe–Co alloys. On the other hand, T_t clearly increases with increasing particle size, suggesting that the fcc phase becomes less stable for larger precipitates. This tendency was observed for another concentration by Monzen and Kato (1992). It is plausible that the increase of the lattice misfit between the precipitate and matrix with increasing particle size gives rise to the instability of the fcc phase in accordance with the concentration dependence of T_t as discussed in a previous subsection.

Acknowledgments

The authors are indebted to Dr H Nakamura for his critical reading of the manuscript and to Mr R Iehara for technical support. This work was supported by a Grant-in-Aid for Scientific Research given by the Ministry of Education, Culture and Sports, Science and Technology of Japan (Grant no 11123219).

References

Abrikosov I A, James P, Eriksson O, Soderlind P, Ruban A V, Skriver H L and Johansson B 1996 *Phys. Rev.* B **54** 3380–4
Ambrose T, Krebs J J, Bussmann K and Prinz G A 1999 *J. Appl. Phys.* **85** 5066–8
Macedo W A A and Keune W 1988 *Phys. Rev. Lett.* **61** 475–8
Monzen R and Kato M 1992 *J. Mater. Sci. Lett.* **11** 56–8
Monzen R, Kato M and Mori T 1989 *Acta Metall.* **37** 3177–82
Muraoka Y, Fujiwara T, Shiga M and Nakamura Y 1981 *J. Phys. Soc. Japan* **50** 3284–91
Nakamura Y, Shiga M and Santa S 1969 *J. Phys. Soc. Japan* **26** 210
Shiga M 1993 *Materials Science and Technology, Electronic and Magnetic Properties of Metals and Ceramics* vol 3B, ed K H J Buschow (Weinheim: VHC) pp 161–210
Tsunoda Y 1988 *J. Phys. F: Met. Phys.* **18** L251–5
——1989 *J. Phys.: Condens. Matter* **1** 10 427–38
Tsunoda Y and Kunitomi N 1988 *J. Phys. F: Met. Phys.* **18** 1405–20
Tsunoda Y, Imada S and Kunitomi N 1988 *J. Phys. F: Met. Phys.* **18** 1421–31
Watanabe Y, Kato M and Saito A 1991 *J. Mater. Sci.* **26** 4307
Weiss R J 1963 *Proc. Phys. Soc.* **82** 281
Zharnikov M, Dittschar A, Kuch W, Meinel K, Schneider C M and Kirschner J 1966 *Thin Solid Films* **275** 262–5